Finite-Difference Time-Domain Method (FDTD) used to simulate Micro-ring resonator for student applications

A. FAZACAS[a,b], P. STERIAN[a*]
[a]*Academic Center for Optical Engineering and Photonics, Faculty of Applied Sciences, University "Politehnica" Bucharest, Romania*
[b]*Institute of Atomic Physics, Magurele, Romania*

In this paper we used the Finite Difference Time-Domain Method (FDTD) to solve Maxwell equations in micro-ring resonator filter. The usefulness of micro-ring resonator has been demonstrated through the variety of applications ranging from optical filters to biological and environmental sensing. Because the transmission spectrum is highly sensitive to the refractive index changes in the surrounding media, these micro-rings were used to detect cancer molecules (University of Illinois). The simulations based on this mathematical model are very suitable to describe the losses in different types of micro-ring resonators. The simulations were made for a single ring and for two rings coupled to a single waveguide at diffrent wavelengths, diffrent refractive index and diffrent widths in order to reduce the losses. It is also described the quality of the coupling for diffrent wavelengths.The obtained result refers to the simulation of amplitude for single resonating micro-ring filters and for multiple micro-rings filters. The object of this paper is to establish that this method can be useful for both designers and students performing numerical simulations as computer experiments.

(Received June 10, 2011; accepted April 11, 2012)

Keywords: micro-ring resonators, microstructure devices, integrated optics, FDTD

1. Introduction

The interest in FDTD Maxwell's equations has increased in the last years which can be seen in the number of published articles [1-13]. The Finite-Diffrence Time-Domain (FDTD) Method is also used in areas such as photonics and nanotechnology. This method is considered easy to understand and easy to implement in software for simulations.

The accuracy of FDTD method is used in simulations for industrial and research design of newly optical components. The modeling of micro-ring resonators is of particular interest, since these devices provide compact, narrow band and large free spectral range of optical channel droping filters. The ratio of optical power coupled between ring and bus waveguides in micro-ring based devices is crucial to the desired device characteristics [6], [11].

Micro-ring resonators are the potential building block integrated circuits and they may be used as electro-optic switches or modulators, in Photonic VLSI circuits or as passive filters for add-drop functions in wavelength-division multiplexing (WDM), for band-stop filtering, for sensing and for optical telecommunications [14-17]. Due to the small size and versatility these micro-rings can be incorporated in integrated optic circuit. Also it can be used to trap microparticles onto silicon micro-ring resonators which have various nanomanipulation applications. [13]

The micro-ring resonator can be manufactured from different materials using E-beam or UV lithography. Most used material is silicon because it has a small absorption loss at telecommunication wavelength of 1.55 μm. Micro-rings based on GaAs materials are used to manufacture high electron mobility transistors. Polymers are also used as manufacture material for micro-rings because of their lower cost and better integration. Such materials are used to manufacture passive devices, electro-optic and thermo-optic devices [18-21].

It was proved that the difference in refractive index between core and cladding will reduce losses, but the fabrication will become more expensive. There have been used a range of different materials in experiments: III-V materials, silicon nitride, Si on insulator and Ge doped silica [6].

In this paper we will simulate the amplitude and for single ring and two rings coupled to a single waveguide. The simulation were made for diffrent wavelengths and diffrent refractive index. In order to achieve these results we used the OptiFDTD Software.

2. Theory

We consider a region of space with no electric or magnetic current sources, but may have materials that absorb electric or magnetic field energy. The time-dependent Maxwell's equations are given by the following equations:

$$\frac{\partial \vec{B}}{\partial t} = -\nabla \times \vec{E} - \vec{M} \; ; \frac{\partial \vec{D}}{\partial t} = \nabla \times \vec{H} - \vec{J} \qquad (1)$$

$$\nabla \cdot \vec{D} = 0 \; ; \; \nabla \cdot \vec{B} = 0 \qquad (2)$$

where $\vec{E}$ is the electric field (V/m), $\vec{D}$ is the electric flux density (C/m^2), $\vec{H}$ is the magnetic field (A/m), $\vec{B}$ is the magnetic flux density (Wb/m^2), and $\vec{J}$ is the electric current density (A/m^2).

We can relate $\vec{D}$ to $\vec{E}$ and $\vec{B}$ to $\vec{H}$ using the relations:

$$\vec{D} = \varepsilon\vec{E} = \varepsilon_r\varepsilon_0\vec{E}\,;\ \vec{B} = \mu\vec{H} = \mu_r\mu_0\vec{H} \tag{3}$$

where ε (F/m), ε_r is the relative permittivity, ε_0 is the free-space permittivity (8.85×10^{-12}), μ is the magnetic permeability (H/m), μ_r is the relative permeability, and μ_0 is the free-space permeability ($4\pi\times10^{-7}$ H/m).

$\vec{J}$ and $\vec{M}$ can act as independent sources of $\vec{E}$ and $\vec{H}$ field energy and can be written as:

$$\vec{J} = \vec{J}_{source} + \sigma\vec{E};\qquad \vec{M} = \vec{M}_{source} + \sigma^*\vec{H} \tag{4}$$

where σ is the electric conductivity (S/m) and σ^* is the magnetic loss (Ω/m).

Using (1), (3) and (4) we obtain the Maxwell's curl equations in linear, isotropic, non-dispersive, lossy materials:

$$\frac{\partial\vec{H}}{\partial t} = -\frac{1}{\mu}\nabla\times\vec{E} - \frac{1}{\mu}\left(\vec{M}_{source} + \sigma^*\vec{H}\right) \tag{6}$$

$$\frac{\partial\vec{E}}{\partial t} = \frac{1}{\varepsilon}\nabla\times\vec{H} - \frac{1}{\varepsilon}\left(\vec{J}_{source} + \sigma\vec{E}\right) \tag{7}$$

If we write the vector components of the curl operators in Cartesian coordinates we will obtain the following system of six coupled scalar equations:

$$\frac{\partial\vec{H}_{x,y,z}}{\partial t} = -\frac{1}{\mu}\left[\frac{\partial E_{y,z,x}}{\partial z,\,x,\,y} - \frac{\partial E_{z,x,y}}{\partial y,\,z,\,x} - \vec{M}_{source_{x,y,z}}\right] \tag{8}$$

$$\frac{\partial\vec{E}_{x,y,z}}{\partial t} = \frac{1}{\varepsilon}\left[\frac{\partial H_{z,x,y}}{\partial y,\,z,\,x} - \frac{\partial H_{y,z,x}}{\partial z,\,x,\,y} - \vec{J}_{source_{x,y,z}}\right], \tag{9}$$

if we consider that σ^* and σ are equal to zero.

The system of six coupled partial differential equations forms the basis of the FDTD numerical algorithm for electromagnetic wave interactions with general three-dimensional objects.

To determine each component of the magnetic and electric fields we can use Yee algorithm which is very well described in [1],[2].

The most well-known configuration for ring resonator consists of a unidirectional coupling between a ring with radius r and a waveguide as we can see in Fig. 1a. There are different types of coupling for micro-ring resonators as we can see in Fig. 1b and Fig. 1c.

Ring coupling relations are given by the following equations:

$$\beta = \frac{2\pi n_{eff}}{\lambda}\,;\ \theta = \frac{4\pi n_{eff}\,r}{\lambda} \tag{10}$$

where β is the propagation constant, n_{eff} is the effective refractive index, λ is the wavelength of the laser, θ is the phase shift per circulation and r is the ring radius measured from the center of the ring to the center of the waveguide.

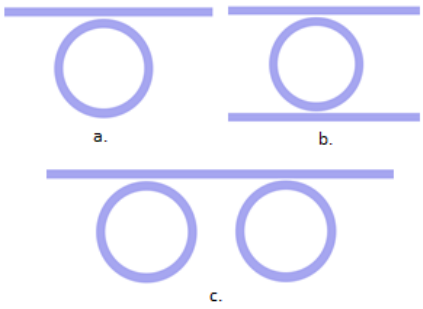

Fig 1. Single ring coupled to (a) single waveguide (b) two waveguides; (c) two rings coupled to single waveguide.

If these rings are used as filters we can describe them with the following parameters:

$$FSR = \frac{\lambda^2}{n_{eff}\,L};\ FWHM = \frac{k^2\lambda^2}{\pi L n_{eff}} \tag{11}$$

$$F = \frac{FSR}{FWHM};\ Q = \frac{n_{eff}}{\lambda}L\cdot F \tag{12}$$

where FSR is the free spectral range, L is the circumference of the ring and k is the vacuum wave number, FWHM – full width half maximum, F is the finesse and Q is the quality factor. The FWHM and FSR are measured as we can see in Fig 2.

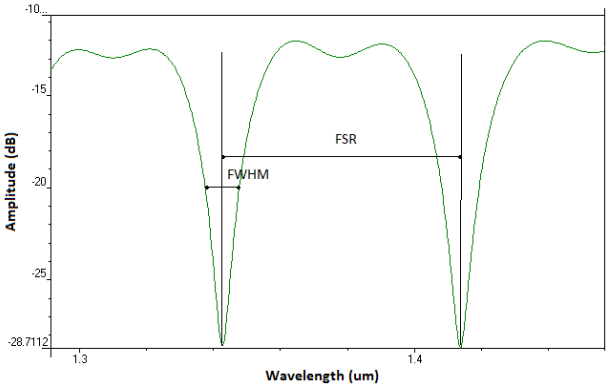

Fig 2. The FWHM is measured at the middle of the resonance peak hight and FSR is measured as the distance between two resonance peaks.

Another important parameter is the mode matching that can be achieved using suitable optics. The quality of mode matching and the coupling efficiency depends upon the overlap integral of the Gaussian mode of the input laser beam and the nearly Gaussian fundamental mode of the fiber. For perfect matching to a cavity mode (typically

the fundamental Gaussian mode), complete transmission of the resonator can be observed when the resonance condition is met, whereas other resonances (corresponding to other resonator modes) cannot be excited [12].

3. Results

First we consider a single ring coupled to a single waveguide with the following parameters: the width of the waveguide is equal to 0.5 μm, the depth 1.25 μm and the length 10 μm; the refractive index of the micro-ring and of the waveguide is constant (Fig.3) in the core and is equal with 2; the refractive index of the cladding is 1; the radius of the micro-ring is 1.7 μm. The separation between micro-ring and waveguide is 0.255 μm.

The wavelength of the laser in simulation is 1.4 μm and the amplitude is 1V/m.

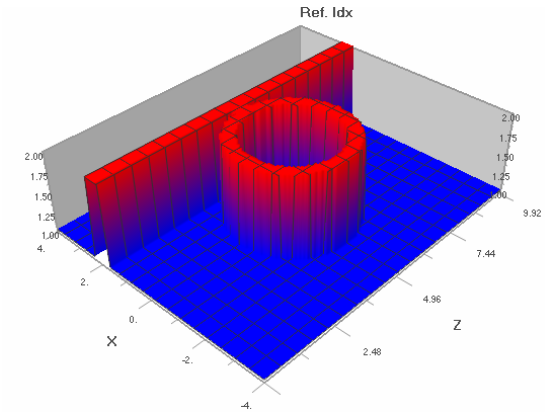

Fig.3 The evolution of refractive index is constant on the waveguide and micro-ring.

We can see in Fig.4a that the amplitude of the ring is lighter than that of the input, but if we increase the wavelength to 1.42 μm (Fig. 4b) or 1.5 μm we can see that the amplitude in the ring is larger than that from the input due to the constructive interference of light in the loops of the ring. At the output of the waveguide, for 1.4 μm we can see that the signal is very close to that from the input. This means that at this wavelength we cannot use the micro-ring as a band-stop filter. For 1.42 μm (Fig.4b) or for 1.5 μm this micro-ring can be used as a band-stop filter at resonance because the signal drops down.

In this simulation we have considered two observation points, one at 0.375 μm and the other one at 9.775 μm. The evolution of amplitude versus the wavelength is plotted in Fig. 5 for the two observation points. At the input we don't have many losses, but at the output we can see that for different wavelength we have smaller or bigger losses. We can also see that indeed this micro-ring can be used as band-stop filter for 1.42 μm, for 1.5 μm and for 1.57 μm.

The FWHM bandwidths at resonances for $\lambda1 = 1.3425$ μm, $\lambda2 = 1.4138$ μm and $\lambda3 = 1.4932$ μm are $\Delta\lambda1 = 0.01$ μm and $\Delta\lambda2 = 0.02$ and μm $\Delta\lambda3 = 0.02$ μm. From these values and using the (11) relation we obtain that Q has values of hundreds. This is not a convenient value for the quality factor.

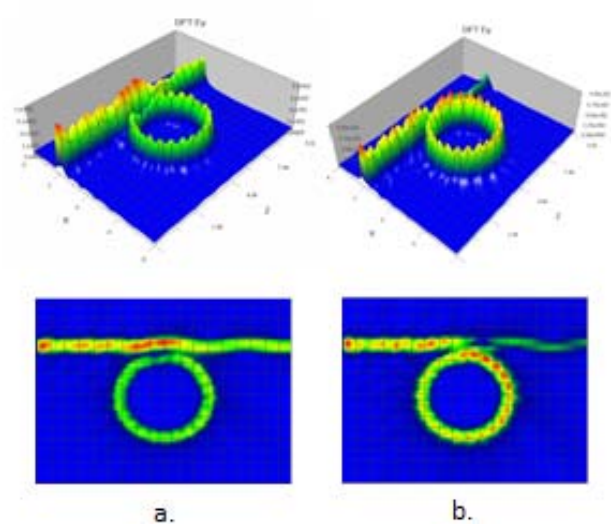

Fig. 4 a. The evolution of Ey component versus distance in 3D and the projection (X, Z axes) in 2D for 1.4 μm; b. The evolution of Ey component versus distance in 3D and the projection (X, Z axes) in 2D for 1.42 μm.

The simulations were made from 1.4 μm to 1.57 μm and we calculate for each wavelength the mode overlap integral at input and at the output of the waveguide.

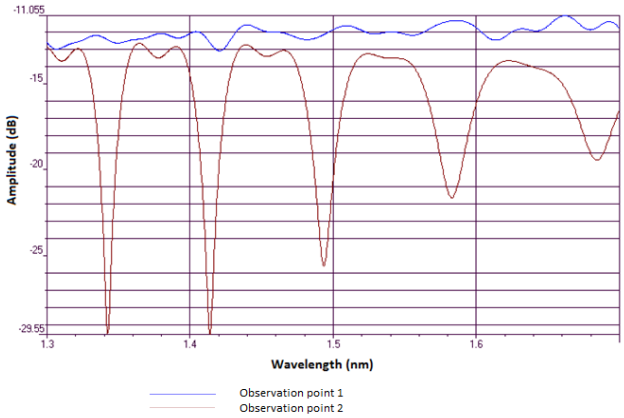

Fig.5 The evolution of amplitude versus wavelength for 2 observation points.

Table 1. Mode Overlap Integral at the input and at the output of the waveguide for different wavelengths

Wavelength (μm)	MO Integral Input (%)	MO Integral Output (%)
1.4	25.0640	30.6492
1.42	20.0915	5.0880
1.45	24.4674	25.9392
1.47	23.2291	27.6093
1.5	22.2932	10.5520
1.52	23.7353	23.6468
1.55	21.7249	24.6228
1.57	22.1811	18.0510

From Table 1 and Fig 6 we can see that at wavelengths where the micro-ring can be used as band-stop filter the mode overlap integrals have smaller values. Higher values of the mode overlap integral means that the coupling efficiency is better.

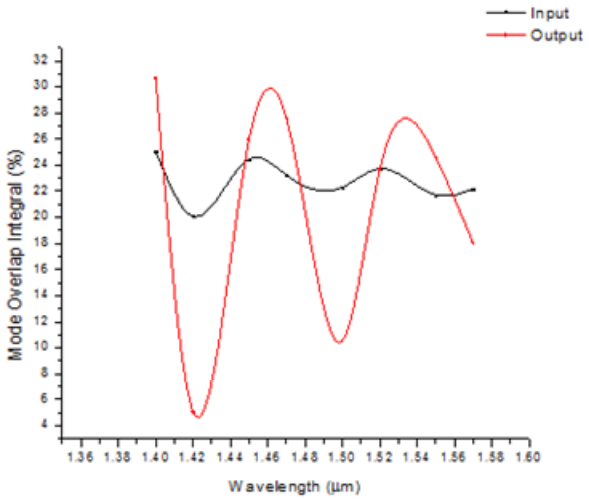

Fig 6 The evolution of mode overlap integral versus wavelength at the input and at the output of the waveguide

If we change the distance between the micro-ring and waveguide to 5.88 µm, we can see that the Ey component changes. In this case we obtain a higher value for the mode overlap integral of 23.94 % , with coupling efficiency improved more than the above ones, but this micro-ring can not be used as band-stop filter.

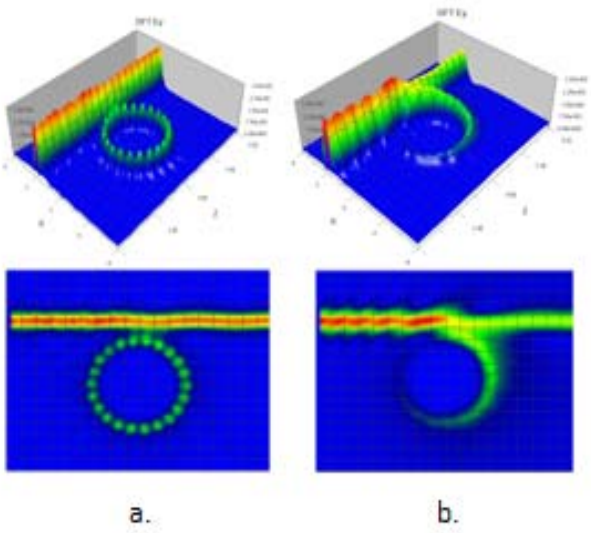

Fig. 7 a. The evolution of Ey component versus distance in 3D and the projection (X, Z axes) in 2D for 1.42 µm and higher separation distance; b. The evolution of Ey component versus distance in 3D and the projection (X, Z axes) in 2D for 1.42 µm and different refractive index.

This change of the refractive index will modify the resonance wavelength as we can see in Fig 8.

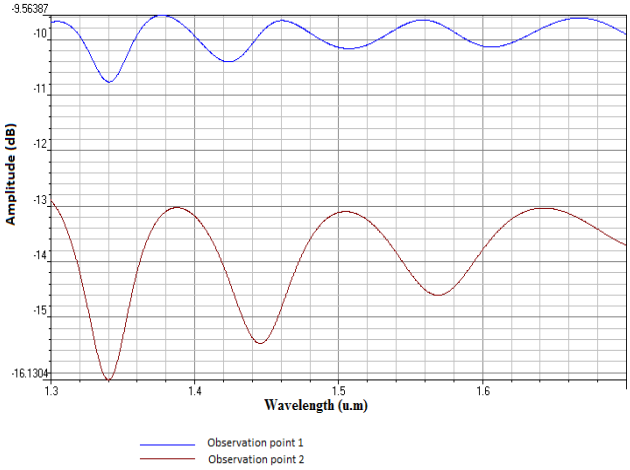

Fig.8 The evolution of amplitude versus wavelength for n = 1.5 and wavelength 1.42 µm .

We made simulation for multiple ring resonators ranging from 1 ring to 5 rings. In this case the signal dissipates through the micro-ring as shown in Fig 9. There is no improvement in the quality factor. In order to improve the quality factor, for better sensing, the resonance wavelength should be sharper.

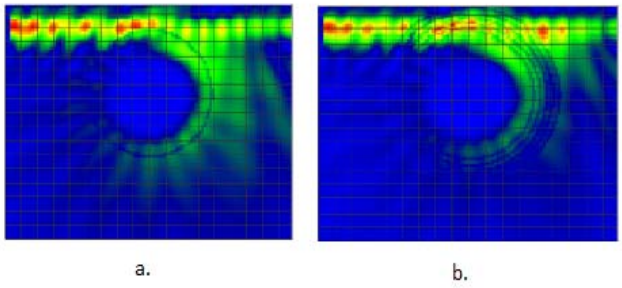

Fig. 9 . The evolution of Ey component versus in 2D for 1.42 µm: a. with one added ring; b. with five added rings

Table 2 and Fig 10 indicate that the amplitude in dB drops with higher values f

Table 2. Variation of amplitude at the output of the waveguide for different number of rings

Number of rings	Amplitude (dB)
1	-12.884400
2	-13.373000
3	-13.659700
4	-13.641100
5	-13.617600

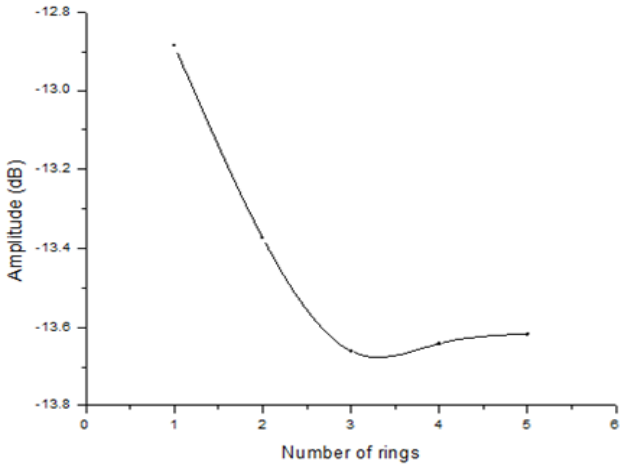

Fig. 10 . The evolution of amplitude at the output of the waveguide for different number of rings.

In order to obtain higher quality factor we made the simulation for a silicon micro-ring on a SiO_2 wafer. We can see in Fig. 11 that the resonance frequencies are sharper and in this case we obtained higher quality factor with values of thousands.

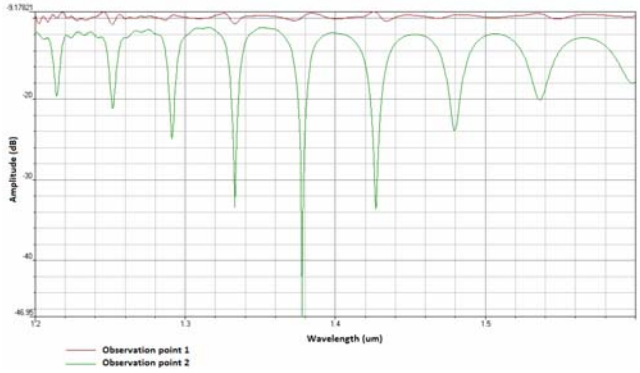

Fig. 11 . The evolution of amplitude versus wavelength for n = 3.49 and wavelength 1.5 μm

4. Conclusions

In conclusion the micro-ring resonators are ideal candidates to manufacture devices ranging from optical filters to lasers. These type of devices can be easily integrated with other semiconductor based devices and show loss variation with the size and with the refractive index.

The Finite Difference Time-Domain Method is a very powerful tool to describe losses in different type of micro-ring resonators. The simulation time is very long (the simulation time, in this study, range from 45 minutes to 8 hours), but the method can be useful for both designers and students performing numerical simulations as computer experiments.

References

[1] Dennis M. Sullivan, Electromagnetic simulations using FDTD Method, Wiley-IEE Press, New York (2000).

[2] Allen Taflove, Susan C. Hagness, Computational Electrodynamics: The Finite-Diffrence Time-Domain Method Second Edition, Artech House INC., London (2000).

[3] Christian Koos, Masafumi Fujii, Christopher G.Poulton, Ralf Steingrueber, Juerg Leuthold, Wolgang Freude, FDTD-Modelling of Dispersive Nonlinear Ring Resonators: Accuracy Studies and Experiments, IEE Journal of Quantum Electronics, **42**(12), 1215 (2006).

[4] S. C. Hagness, D. Rafizadeh, S. T. Ho, A. Taflove, FDTD Microcavity Simulations: Design and Experimental Realization of Waveguide-Coupled Single-Mode Ring and Whispering-Gallery-Mode Disk Resonators, Journal of Lightwave Technology, **15**(11), 2154 (2007).

[5] Ikuo Awai and Yangjun Zhang, Copling Coefficient of Resonators – An Intuitive way of Its Understanding, Electronics and Communications in Japan, Part 2, **90**(9), 962 (2007).

[6] Alastair D.McAulay, Michael R.Corcoran, Christopher J.Florio, and Ian B.Murray, Optical micro-ring resonator filter design trade-offs, Proceedings of SPIE Active and Passive Optical Components for WDM Communications IV, 2004, p. 359.

[7] Vittorio M.N. Passaro, Francesco Dell Olio, Francesco De Leonardis, Ammonia Optical Sensing by Micro-ring Resonators, Sensors, 2007, p 2741.

[8] E.V. Bekker, V.Brulis, D.Gallagher, Accurate Design of Optical Micro-ring Resonators, E.V. Bekker, V.Brulis, D.Gallagher, www.photond.com/ files/docs/ **Bekker**_ECIO2010.pdf , March 2011

[9] Andrzej Kazmierczak, & all, High quality optical micro-ring resonators in Si_3N_4/SiO_2, https://eeweb01.ee.kth.se/upload/publications/... /IR-EE-MST_2008_016.pdf , March 2011

[10] Qianfan Xu and Michal Lipson, Optic Express **15**(3), 924 (2007).

[11] Greeshma Gupta, Micro-ring Resonator based Filters and Modulators: Optical Coupling Control and Applications to Digital Communications, http://digitallibrary.usc.edu/assetserver/controller /item/etd-Gupta-20080509.pdf, March 2011

[12] www.rp-photonics.com/mode_matching.html, March 2011

[13] Shiyun Lin, Ethan Schonbrun, and Kenneth Crozier, Optical Manipulation with Planar Silicon Micro-ring Resonators, Nano Letters, 2010, p. 2408.

[14] E. N. Stefanescu, et al, ALT'02, International Conference on Advanced Laser Technologies, Adelboden- Switzerland, Proc. SPIE, **5147**, 160 **(**2003).

[15] A. Sterian, "Computer modeling of the coherent optical amplifier and laser systems", Editor(s): Gervasi,O; Gavrilova, ML., Computational Science and Its Applications - ICCSA 2007, Pt 1, Proceedings 4705436-449, (2007).
[16] A. R. SterianAdvances in Optical Amplifiers, Paul Urquhart (Ed.), ISBN: 978-953-307-186-2, InTech,VIENNA (2011).
[17] F. C. Maciuc, et al Proceedings of SPIE, Laser Physics and Applications, **4394**, 84 (2001).
[18] E. N. Stefanescu, et al..: Proceedings of SPIE, **5850**, 160-165 (2005).
[19] M. Dima, M. Dulea, D. Aranghel et al., Optoelectron. Adv. Mater. – Rapid Commun. **4**(11), 1840 (2010).
[20] C. Iliescu, M. Avram, B. Chen, et al., J. Optoelectron. Adv. Mater. **13**(2-4), 387 (2011).
[21] D. Mihalache, J. Optoelectron. Adv. Mater. **13**(9), 1055 (2011).

*Corresponding author: a.fazacas@ifa-mg.ro